SWAY AND YAW MOTION CONTROL DUE TO RELUCTANCE FORCE IN CONTROLLED-PM LSM MAGLEV CARRIER

Kinjiro Yoshida*, Hiroshi Takami*, Yasunori Nakahashi**, Kenji Shimamoto*

* Department of Electrical and Electronic System Engineering,
Graduate School of Information Science and Electrical Engineering,
Kyushu University
10-1 6-chome Hakozaki Higashi-ku Fukuoka ,812-8581 Japan

** Fuji Electric CO.,LTD

SUMMARY

In controlled-PM LSM Maglev Carrier, four attractive-forces of four controlled-PM's fixed rigidly on the carrier can control heave, pitch and roll motions, by using an integral-control method. We have completed minimizing of electric power loss for its levitation. But it is very difficult to control guidance with the sway and yaw motions without any additional magnets and coils. For guidance control we have made successful use of a lateral reluctance-force which is produced between controlled-PM and armature iron rail.

INTRODUCTION

An experimental Maglev carrier in our laboratory (Fig. 1) has four controlled-PM's (CPM's) arranged rigidly at the four corners on the same plane of the bogie [1]. It is impossible to apply the local control method to the levitation problem for controlling simultaneously the four CPM's in the Maglev carrier system which includes six degrees of freedom. The integrated control method should be used to design the robust levitation control system for minimizing the electric power loss. The levitation control at standstill and propulsion motion combined with levitation have been carried out in our previous research without guidance control [2], [3]. The five degrees of freedom except propulsion motion can be controlled independently of the propulsion motion. The propulsion force due to LSM is treated as a disturbance for the heave, pitch, roll, sway and yaw motions. To control guidance with sway and yaw motions, a lateral force is required [4]. A reluctance force between CPM and armature iron rail can be used effectively.

This paper proposes a simple control method of using only *four* CPM's for the *five* degrees of freedom including sway and yaw motions as well as heave, pitch and roll ones. The method is based on using the lateral reluctance-force which is produced at both side-edges between CPM and armature iron rail. The restoring reluctance force is produced without any additional magnets and coils and depends on lateral displacement, airgap length and PM control current.

DYNAMICS MODELING OF MAGLEV CARRIER

Figure 1 shows a configuration of controlled-PM LSM Maglev Carrier in which the 2-pole-controlled PM's are arranged rigidly at the four corners on the same plane. The LSM armature guideway is also constructed rigidly. The levitation control system levitates the carrier stably while the propulsion control system propels the carrier by synchronizing the CPM with the travelling magnetic field produced by the stator armature current-carrying windings.

Figure 2 shows a rigid bogie model of Maglev carrier which has six degrees of freedom [5]. The heave motion is described as that of the center of the gravity (CG):

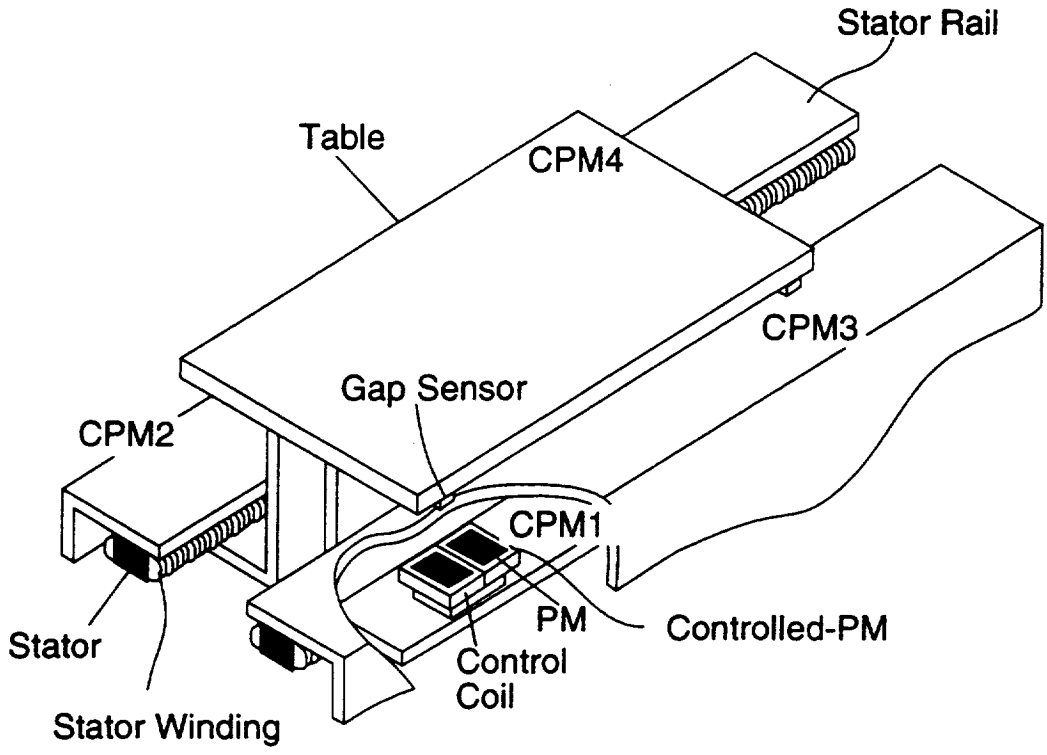

Figure 1. Controlled-PM Maglev Carrier.

$$M\frac{d^2\Delta h_{Gz}}{dt^2} = F_{z1} + F_{z2} + F_{z3} + F_{z4} - Mg + F_{z,ex} \tag{1}$$

where M = the mass of carrier

h_{Gz} = the height of the CG with respect to the reference plane, which is defined in the downward direction as shown in Fig.2

$F_{zi}(i = 1,2,3,4)$ = the lift force produced in the CPM i (i = 1,2,3,4)

$F_{z,ex}$ = the external force, such as aerodynamic drag force, and g is the acceleration of gravity

The roll motion is described as

$$I_\theta \frac{d^2\theta}{dt^2} = (F_{z1} - F_{z2} + F_{z3} - F_{z4})l_y - (F_{y1} + F_{y2} + F_{y3} + F_{y4})l_z + N_{\theta,ex} \tag{2}$$

where I_θ = the moment of inertia around the x-axis

θ = the roll angle, l_y and l_z the y- and z- directed distance between the CG and the PM's

$F_{yi}(i = 1,2,3,4)$ = the guide force produced in the CPM i (i = 1,2,3,4), [4]

$N_{\theta,ex}$ = the external moment around the x-axis

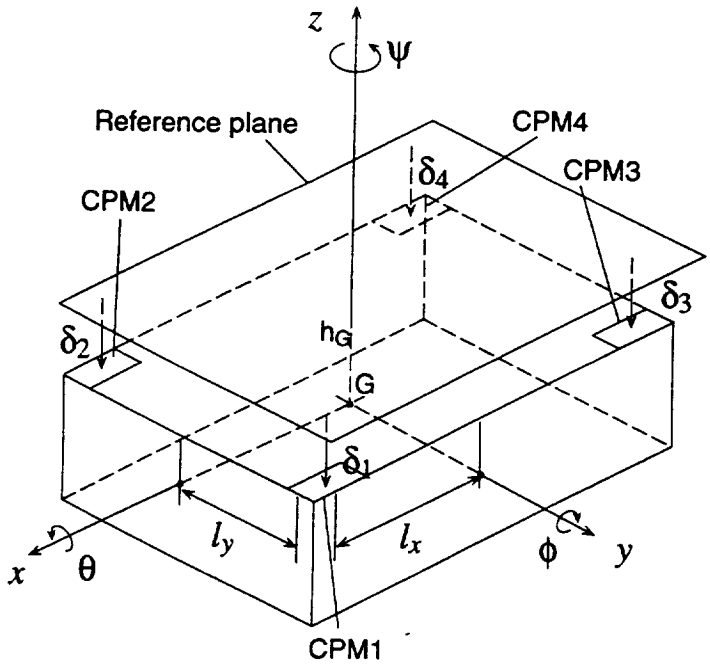

Figure 2. Rigid bogie model of carrier.

The pitch motion is described as

$$I_{\phi}\frac{d^2\phi}{dt^2}=(-F_{z1}-F_{z2}-F_{z3}+F_{z4})l_x+(F_{x1}+F_{x2}+F_{x3}+F_{x4})l_z+N_{\phi.ex} \tag{3}$$

where I_{ϕ} = the moment of inertia around the y-axis
ϕ = the pitch angle
F_{xi} (i = 1,2,3,4) = the thrust force produced in the CPMi (i = 1,2,3,4)
l_x = the x-directed distances between the CG and the PM's
$N_{\phi.ex}$ = the external moment around the y-axis

It is clear that equation (3) includes explicitly propulsion forces F_{xi} (i = 1,2,3,4) and the pitch motion is affected directly by F_{xi} (i = 1,2,3,4).

The sway motion is described as

$$M\frac{d^2\Delta h_{Gy}}{dt^2}=F_{y1}+F_{y2}+F_{y3}+F_{y4}+F_{y.ex} \tag{4}$$

where h_{Gy} = the sway position of the CG with respect to the reference point
$F_{y.ex}$ = the external force

The yaw motion is described as

$$I_{\psi}\frac{d^2\psi}{dt^2}=(-F_{x1}+F_{x2}-F_{x3}+F_{x4})l_y+(F_{y1}+F_{y2}-F_{y3}-F_{y4})l_x+N_{\psi.ex} \tag{5}$$

where I_{ψ} = the moment of inertia around the z-axis
ψ = the yaw angle
$N_{\psi.ex}$ = the external moment around the z-axis

The self-inductance L_2 of the CPM coils are very large compared with the mutual inductance M between them and armature coils, so that terms associated with M can be neglected in the circuit equations of levitation control coils. They are described as

$$L_2\dot{I}_{2i}+K_{\delta}\dot{\delta}_i+R_2I_{2i}=e_{ci}\quad(i=1,2,3,4) \tag{6}$$

where

I_{2i} $(i = 1,2,3,4)$ = an instantaneous current of the CPMi ($i = 1,2,3,4$) coils
K_{δ} = the speed EMF coefficient due to the change in airgap
R_2 = the equivalent resistance of control coil including additional resistance
e_{ci} $(i = 1,2,3,4)$ = the control voltage supplied to stabilize the levitation system according to the integrated control law

INTEGRATED-CONTROL DESIGN FOR MAGLEV CARRIER

At standstill when the Maglev carrier has no propulsion forces, i.e.$F_{xi} = 0$, the mutually cross-coupling levitation motion described by equations (1) - (5) and following equations (7) (8) that express the relationships of the airgaps δ_i between Δh_g, θ, ϕ and y_i between h_{Gy}, ψ can be transformed into five independent motions of the heave, roll, pitch, sway and yaw. They are expressed as follows.

$$\begin{bmatrix}\Delta\delta_1\\ \Delta\delta_2\\ \Delta\delta_3\\ \Delta\delta_4\end{bmatrix} = -\begin{bmatrix}1 & 1 & -1 & -1\\ 1 & -1 & -1 & 1\\ 1 & 1 & 1 & 1\\ 1 & -1 & 1 & -1\end{bmatrix}\begin{bmatrix}\Delta h_{Gy}\\ l_Y\theta\\ l_X\phi\\ 0\end{bmatrix} = -T_1^{\mathrm{T}}\begin{bmatrix}x_G\\ x_\theta\\ x_\phi\\ 0\end{bmatrix} \tag{7}$$

$$\begin{bmatrix}\Delta y_1\\ \Delta y_2\\ \Delta y_3\\ \Delta y_4\end{bmatrix} = -\begin{bmatrix}-1 & -1 & -1 & 1\\ -1 & -1 & 1 & -1\\ -1 & 1 & -1 & -1\\ -1 & 1 & 1 & 1\end{bmatrix}\begin{bmatrix}h_{Gy}\\ r\psi\\ 0\\ 0\end{bmatrix} = -T_2^{\mathrm{T}}\begin{bmatrix}h_{Gy}\\ r\psi\\ 0\\ 0\end{bmatrix} \tag{8}$$

$$M\frac{d^2\Delta h_{Gz}}{dt^2} = F_{Gz} - Mg + F_{z.ex} \tag{9}$$

$$I_\theta\frac{d^2\theta}{dt^2} = F_{G\theta}l_y + F_{\theta.ex} \tag{10}$$

$$I_\phi\frac{d^2\phi}{dt^2} = F_{G\phi}l_y + F_{\phi.ex} \tag{11}$$

$$M\frac{d^2\Delta h_{Gy}}{dt^2} = F_{Gy} + F_{y.ex} \tag{12}$$

$$I_{\psi}\frac{d^2\psi}{dt^2} = F_{G\psi}\sqrt{l_x^{\,2}+l_y^{\,2}} + F_{\psi,ex} \tag{13}$$

where F_{ZGz}, $F_{Z\theta}$, $F_{Z\phi}$, F_{YGy}, $F_{Y\psi}$ are derived from

$$\begin{aligned}&\left[F_{ZGz} \quad F_{Z\theta} \quad F_{Z\phi} \quad F_{ZV} \quad F_{YGy} \quad F_{Y\psi} \quad F_{YU} \quad F_{YW}\right]^{T}\\ &\quad = T\left[F_{Z1} \quad F_{Z2} \quad F_{Z3} \quad F_{Z4} \quad F_{Y1} \quad F_{Y2} \quad F_{Y3} \quad F_{Y4}\right]^{T}\end{aligned} \tag{14}$$

by using the following transformation matrix

$$T = \begin{bmatrix} T_1 & 0 \\ 0 & T_2 \end{bmatrix} \tag{15}$$

The linearizing equations (9) - (13) around the nominal operating point of $\delta_i = \delta_0$ (i = 1,2,3,4), I_{2i} = 0 (i = 1,2,3,4), the subsystem is obtained in the form of

$$M_j\frac{d^2X_j}{dt^2} = -4K_{FD}X_j + K_{FI}I_{2j} + F_{j,ex} \qquad \left(j = G_z,\theta,\phi,G_y,\psi\right) \tag{16}$$

where

$$k_{FD} = \left(\frac{\partial F_z}{\partial \delta}\right)_{\delta=\delta_0, I_2=0}, \quad k_{FI} = \left(\frac{\partial F_z}{\partial I_z}\right)_{\delta=\delta_0, I_2=0}$$

$$X_{Gz} = \Delta h_{Gz}, \quad X_{\theta} = l_y\theta, \quad X_{\phi} = l_x\phi$$

$$X_{Gy} = \Delta h_{Gy}, \quad X_{\psi} = \sqrt{l_x^{\,2}+l_y^{\,2}}\,\psi$$

$$M_{Gz} = M, \quad M_{\theta} = I_{\theta}l_y^{-2}, \quad M_{\phi} = I_{\phi}l_x^{-2} \tag{17}$$

$$M_{Gy} = M, \quad M_{\psi} = I_{\psi}\sqrt{l_x^{\,2}+l_y^{\,2}}^{-2}$$

$$\begin{aligned}&\left[I_{2Gz} \quad I_{2\theta} \quad I_{2\phi} \quad I_{2V} \quad I_{2Gy} \quad I_{2\psi} \quad I_{2U} \quad I_{2W}\right]^{T}\\ &\quad = T\left[I_{2z1} \quad I_{2z2} \quad I_{2z3} \quad I_{2z4} \quad I_{2y1} \quad I_{2y2} \quad I_{2y3} \quad I_{2y4}\right]^{T}\end{aligned}$$

In the same manner, the circuit equation (6) of the levitation system are given by

$$L_2 \frac{dI_{2j}}{dt} - 4k_\delta \frac{dx_j}{dt} + R_2 I_{2j} = e_{cj} \qquad (j = G_z, \theta, \phi, G_y, \psi) \tag{18}$$

$$L_2 \frac{dI_{2j}}{dt} + R_2 I_{2j} = e_{cj} \qquad (j = U, V, W) \tag{19}$$

where

$$\begin{bmatrix} e_{cGz} & e_{c\theta} & e_{c\phi} & e_{cV} & e_{cGy} & e_{c\psi} & e_{cU} & e_{cW} \end{bmatrix}^T = T \begin{bmatrix} e_{cz1} & e_{cz2} & e_{cz3} & e_{cz4} & e_{cy1} & e_{cy2} & e_{cy3} & e_{cy4} \end{bmatrix}^T \tag{20}$$

Equations (16) and (18) are three subsystems expressed as

$$\frac{dx_j}{dt} = A_j x_j + B_j u_j + d_j \qquad \left(j = G_z, \theta, \phi, G_y, \psi\right) \tag{21}$$

$$x_j = \begin{bmatrix} x_j & \dot{x}_j & I_{2j} \end{bmatrix}^T, \qquad u_j = e_{cj} \tag{22}$$

$$A_j = \begin{bmatrix} 0 & 1 & 0 \\ -4k_{FD}/M_j & 0 & K_{FI}/M_j \\ 0 & 4k_\delta / L_2 & -R_2 / L_2 \end{bmatrix} \tag{23}$$

$$B_j = \begin{bmatrix} 0 & 0 & 1/L_2 \end{bmatrix}^T \tag{24}$$

Therefore, for each mode of motions, a stable levitation-control system is designed by applying the theory of linear optimal control.

DIGITAL CONTROL SYSTEM DESIGN

For the experimental Maglev carrier, an optimal digital levitation control system is designed to minimize the power loss in the control circuit. By descretizing the continuous subsystems of equation (21) by means of zero-hold with a sampling time, 1 type digital servosystem for three independent-motions are constructed as shown in Fig.3. Feedback gains K_1, K_2 and K_3 are determined from optimizing the following performance index

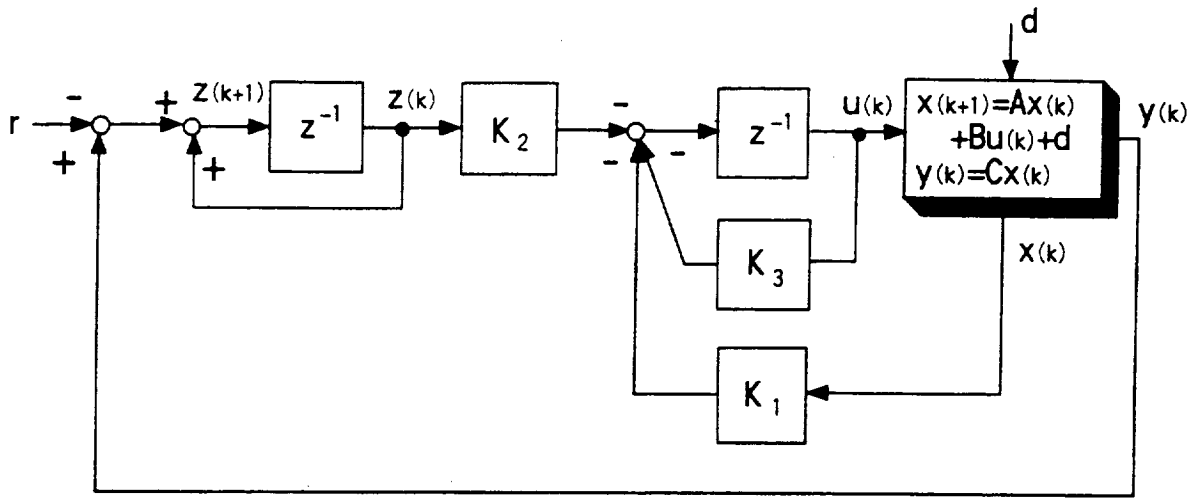

Figure 3. Servo system counting for sampling time.

$$J=\sum_{k=0}^{\infty}\left\{\delta\mathbf{X}(k)Q^{T}\delta\mathbf{X}(k)+\delta\mathbf{u}(k+2)R^{T}\delta\mathbf{u}(k+2)\right\} \tag{25}$$

where

$\delta\ \boldsymbol{X}$(k), $\delta\ \boldsymbol{u}$(k) = deflections from the steady-state values of $\boldsymbol{X}$ and $\boldsymbol{u}$

$\boldsymbol{Q}$, $\boldsymbol{R}$ = weighting coefficient matrices

The digital control algorithm for minimizing levitation loss is achieved by choosing $\boldsymbol{c}$ = [0 0 1] and outputs $y_j = I_{2j}$ ($j = G_z,\ \theta\ ,\ \phi\ ,G_y,\ \psi$). The control laws corresponding to the CPMi (i = 1,2,3,4) are given by putting $e_{cv} = 0$ and by transforming inversely e_{cj} ($j = G_z,\ \theta\ ,\ \phi\ ,G_y,\ \psi$) by the help of the transformation matrix T, as follows:

$$\begin{aligned} e_{ci}(k+1) &= K_{z1}\Delta\boldsymbol{\delta}(k)+K_{z2}\Delta\dot{\boldsymbol{\delta}}(k) \\ &\quad -K_{z3}I_{2i}(k)-K_{z4}\sum I_{2i}(n)-K_{z5}e_{ci}(k) \end{aligned} \qquad (i = 1,2,3,4) \tag{26}$$

where

K_{zm} (m = 1,2,3,4,5) = control gain matrices

$\Delta\boldsymbol{\delta}(k)=\left[\Delta\delta_1(k)\ \ \Delta\delta_2(k)\ \ \Delta\delta_3(k)\ \ \Delta\delta_4(k)\right]^{T}$

SWAY AND YAW MOTION CONTROL STRATEGY AND DESIGN

Sway and yaw motions in phase of stable levitation of Maglev carrier can be damped by controlling reluctance force between stator iron and CPM's. The reluctance force is dependent on lateral displacement,

airgap length and PM control current [4]. When lateral displacement is increased with sway motion, a method to brake it effectively is to decrease airgap length and to increase control current. With respect to yaw motion, it is also true. However it is a problem how to do that by means of four lateral displacement y_i ($i = 1, 2, 3, 4$) caused due to sway and yaw motions. From some experiments, we have found a simple control method given in following equation:

$$\Delta e_{ci}(k+1) = \sum_{v=1}^{4} \{K_{Y1} \Delta y_v(k) + K_{Y2} \Delta \dot{y}_v(k)\} \qquad (i = 1, 2, 3, 4) \tag{27}$$

where

$K_{Yi} (i = 1,2,3,4)$ = control gain for sway-motion control which is obtained by integrated control method
$\Delta y_i (i = 1,2,3,4)$ = lateral displacement of each CPM center of LSM guideway
$\Delta \dot{y}_i (i = 1,2,3,4)$ = speed of lateral displacement of each CPM

Equation (27) is superposed on equation (26).

LEVITATION AND GUIDANCE CONTROL SYSTEM FOR EXPERIMENT

Figure 4 shows a configuration of levitation and guidance control system for the experiments. The gaps and current information from eight gap-sensors and four current-sensors are fed as a form of voltage to personal computer through A/D converters. The required control-voltages for each CPM's are calculated by personal computer according to equation (26). The control coil current is supplied with a sampling time of 1 ms by the PWM controllers.

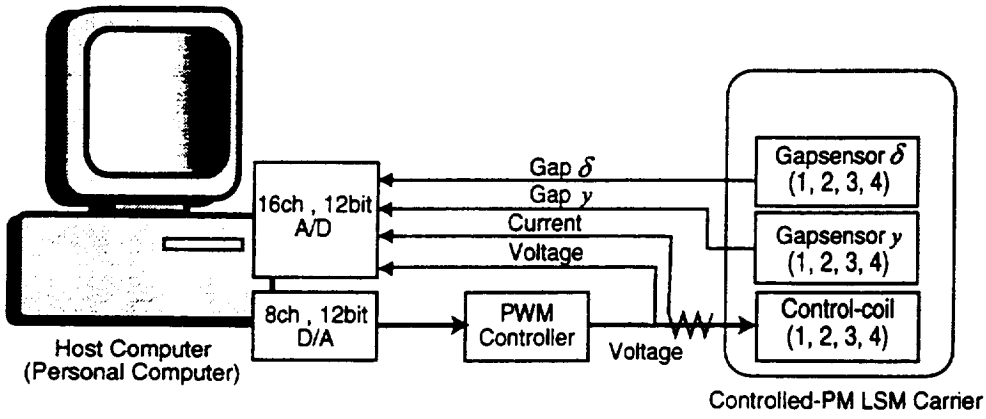

Figure 4. Levitation control system for experiment.

SWAY AND YAW CONTROL EXPERIMENTS

Figure 5 shows the experimental results of sway-and-yaw control by utilizing the lateral reluctance-force between CPM and armature iron rail during Maglev motion. The carrier takes off from initial height of 0.45mm limited mechanically by guide rollers and initial sway of about -2.2mm, and levitates at the standstill and stops from Maglev condition. Maximum control current is limited about 30A. Three-step-sway-control synchronizing the variation of sway motion is carried out effectively in order to suppress sway and yaw motions. Figures 5 (a) and (b) show the sway and yaw motions with sway-control (solid lines) and without sway-control (dotted line) *i.e.* free dynamics of sway and yaw motions, respectively. The halftone regions in the figures indicate intervals during which sway motion is controlled. Each control is started from a negative maximum value of sway motions and finished with 1.5 cycles of its oscillation. Though yaw motion becomes relatively large in only the regions of sway control, the sway and yaw motions are damped rapidly and the excellent sway-and-yaw motion control is achieved. On the other hand, sway and yaw motions without the control are oscillated continuously. Figures 5 (c) and (d) show control current i_{21} of CPM1 and heave motion h_{Gz}, respectively. In the sway control region, the control current and heave motion are varied similarly to oscillation of sway motion. Figures 5 (e) and (f) show the roll motion θ and pitch motion ϕ, respectively. Variations of these motions are very small and stable levitation control of carrier is realized and those with and without sway control are almost the same.The roll and pitch motions with sway control correspond almost to those without sway control. Figures 5 (g) - (i) show the control currents of CPM2, CPM3 and CPM4. These waveforms are the same as those in Fig.5 (c).

CONCLUSIONS

A simple control method for the five degrees of freedom including sway and yaw motions as well as heave, pitch and roll motions have been proposed for controlled-PM LSM Maglev carrier in our laboratory. By using the lateral reluctance-force which is produced at both side-edges between CPM and armature iron rail, oscillations of sway and yaw motions have been damped successfully by experiments without any additional magnets and coils. The results in this research leads to practical Maglev carrier system.

REFERENCES

1. K.Yoshida, E.Zen, H.Inoguchi, S.Sonoda and T.Nakano : Lift Force Analysis in a Controlled-PM LSM Maglev Carrier, Proc. of Int. Conf. on Magnetic Bearings, zurich June 1988, pp.103-163

2. K.Yoshida, T.Yamashita and T.Jyozaki : Dynamics of Controlled-PM LSM Maglev Carrier, Proc. of the 4th Sym. on Dynamics related to Electromagnetic Forces, Invited 5-1, June 1992, pp.93-99

3. K.Yoshida, H.Takami, A.Hasuike, T.Hirakawa, J.Lee, T.Omura, A.Sonoda : Levitation and Pro pulsion motion control of Controlled-PM LSM Maglev Carrier, Proc. of Inter. Conf. on Electrical Machines, Sept. 1994, Vol.2, pp.21-26

4. K.Yoshida, J.Lee, T.Omura : Performance Analysis of Controlled-PM LSM Maglev Carrier with Lateral Displacement by 3-D FEM, Proc. of Int. Conf. on Linear Drives and Industry Application, May 1995, PP.215-218

5. K.Yoshida, T.Omura, J.Lee : Dynamics Simulations of Controlled-PM LSM Maglev Carrier, Taking into account Six Degree of Freedom, Advanced Computational and Design Techniques in Applied Electromagnetic Systems (book), 1995, Elsevier, PP.391-394

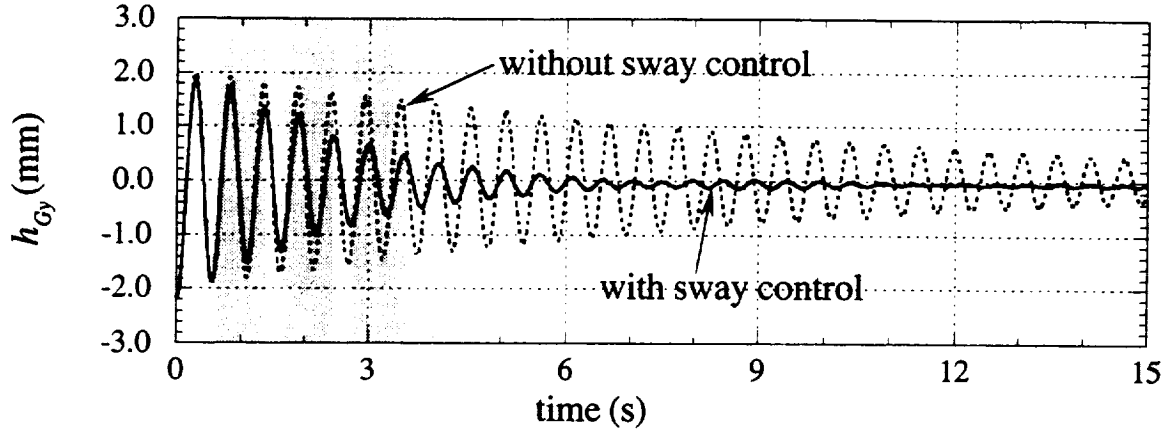

(a) Sway motion

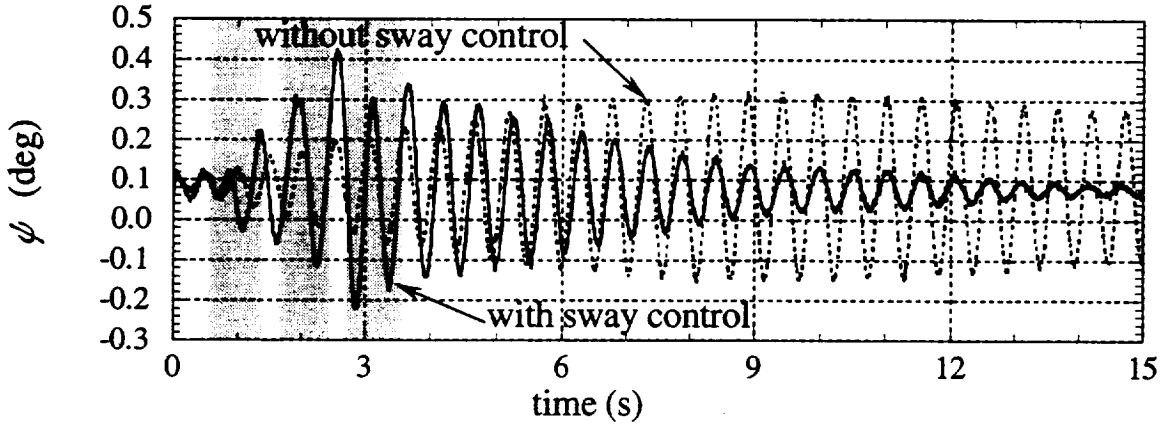

(b) Yaw motion

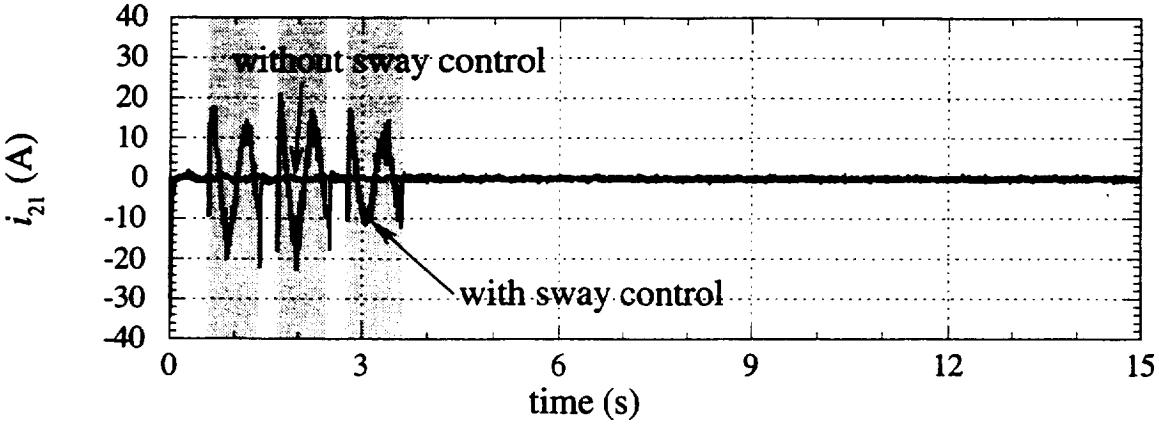

(c) Control current i_{21}

Figure 5. Experimental Results.

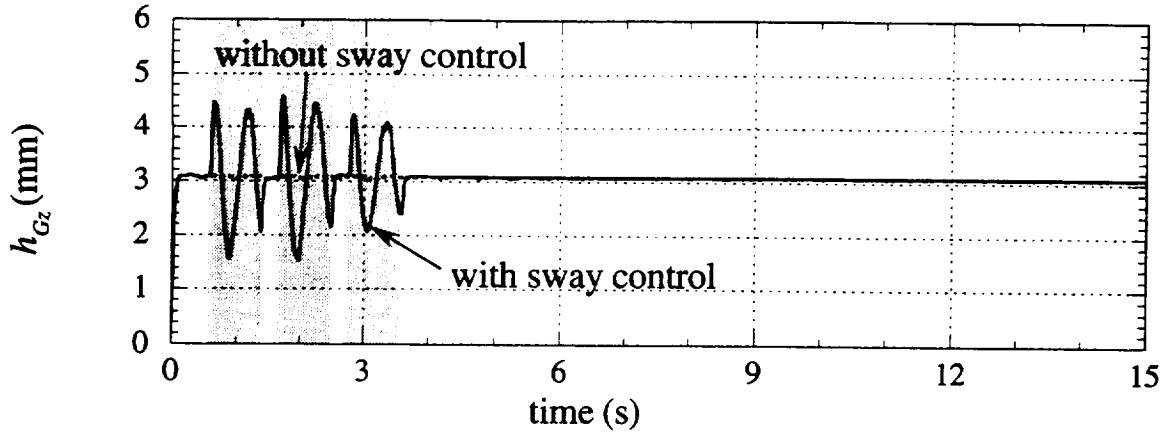

(d) Heave motion

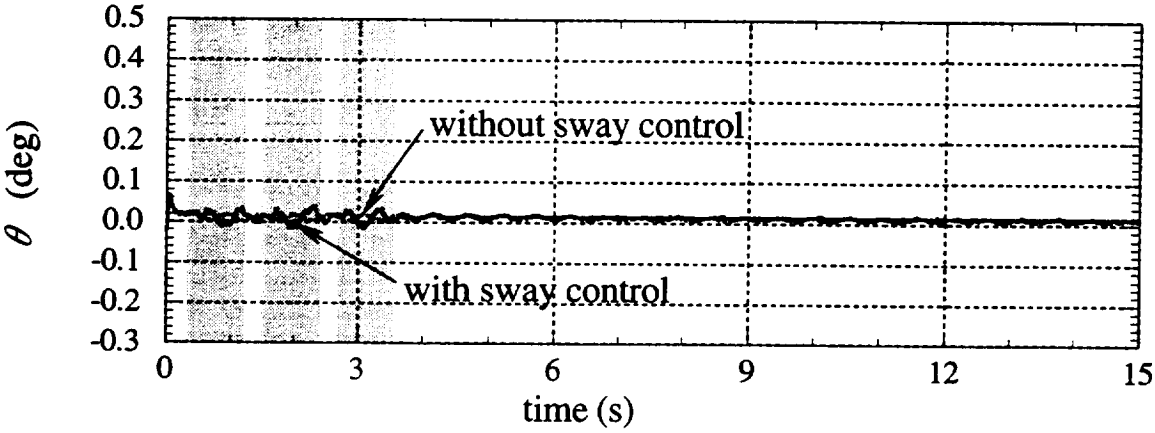

(e) Roll motion

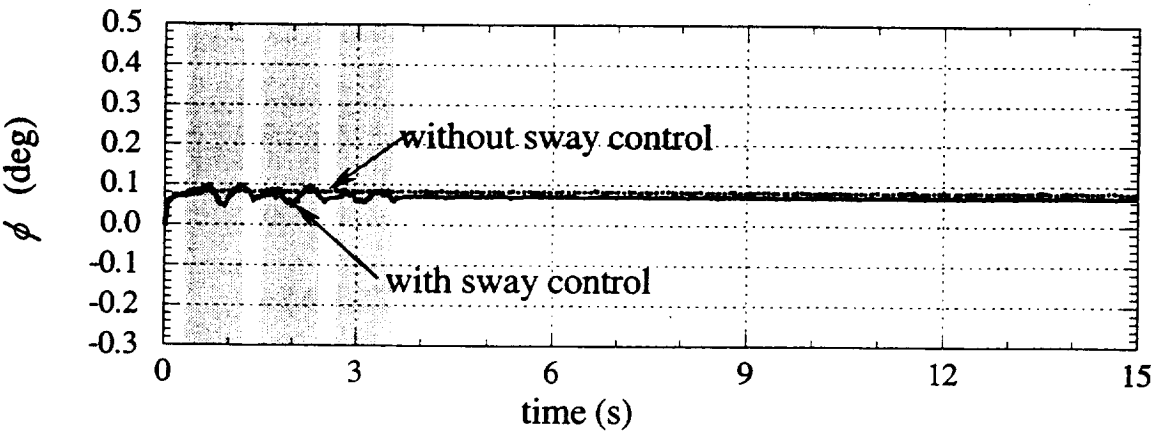

(f) Pitch motion

Figure 5. Experimental Results (cont.)

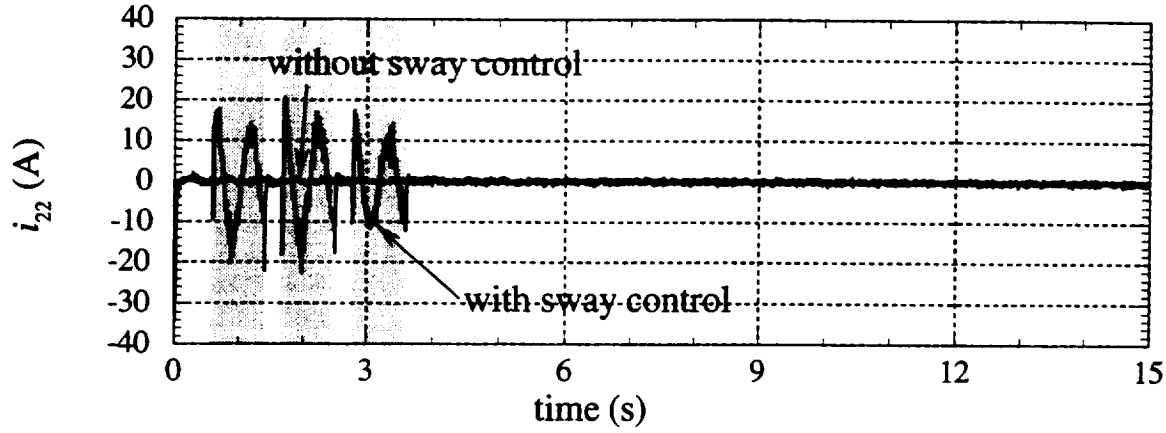

(g) Control current i_{22}

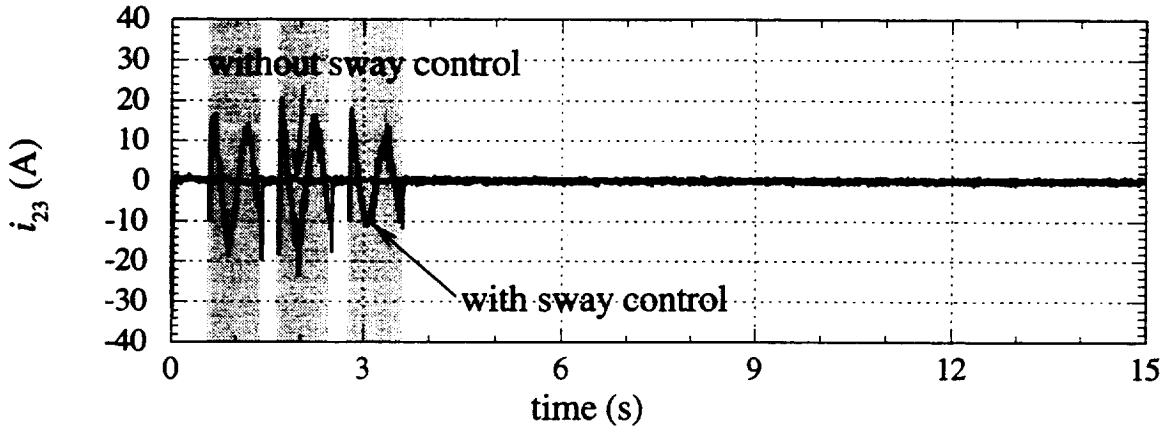

(h) Control current i_{23}

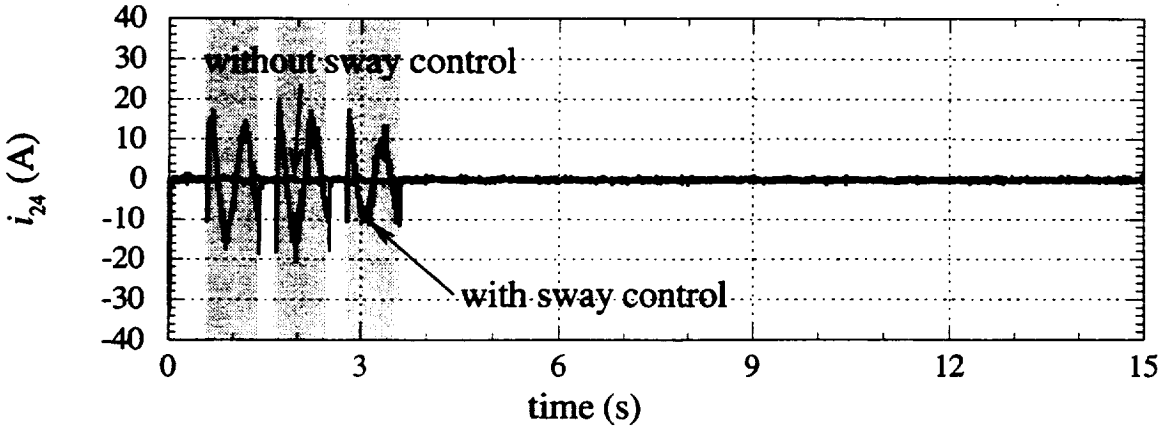

(i) Control current i_{24}

Figure 5. Experimental Results (cont.)